European Journal of Medicinal Chemistry xxx (2014) 1–8

Contents lists available at ScienceDirect

European Journal of Medicinal Chemistry

journal homepage: http://www.elsevier.com/locate/ejmech

Original article

Inhibition of the HIF1α-p300 interaction by quinone- and indandione-mediated ejection of structural Zn(II)

Madura K.P. Jayatunga [a], Sam Thompson [a], Tawnya C. McKee [b], Mun Chiang Chan [a], Kelie M. Reece [c], Adam P. Hardy [a], Rok Sekirnik [a], Peter T. Seden [a], Kristina M. Cook [c], James B. McMahon [b], William D. Figg [c, *], Christopher J. Schofield [a, *], Andrew D. Hamilton [a, *]

[a] Department of Chemistry, Chemistry Research Laboratory, University of Oxford, Oxford OX1 3TA, United Kingdom
[b] Center for Cancer Research, Molecular Targets Laboratory, Frederick National Laboratory Cancer Research, Frederick, MD 21702, USA
[c] NCI, Mol. Pharmacol. Sect., Med. Oncol. Branch, Ctr. Canc. Res., NIH, Bldg. 10, Room 5A01, 9000 Rockville Pike, Bethesda, MD 20892, USA

ARTICLE INFO

Article history:
Received 11 February 2014
Accepted 3 June 2014
Available online xxx

Keywords:
Hypoxia
HIF
p300/CBP
Zinc ejection
Electrophile
Quinone

ABSTRACT

Protein–protein interactions between the hypoxia inducible factor (HIF) and the transcriptional coactivators p300/CBP are potential cancer targets due to their role in the hypoxic response. A natural product based screen led to the identification of indandione and benzoquinone derivatives that reduce the tight interaction between a HIF-1α fragment and the CH1 domain of p300. The indandione derivatives were shown to fragment to give ninhydrin, which was identified as the active species. Both the naphthoquinones and ninhydrin were observed to induce Zn(II) ejection from p300 and the catalytic domain of the histone demethylase KDM4A. Together with previous reports on the effects of related compounds on HIF-1α and other systems, the results suggest that care should be taken in interpreting biological results obtained with highly electrophilic/thiol modifying compounds.

1. Introduction

In humans and other animals the hypoxia inducible factor (HIF) system plays a central role in the hypoxic response [1–4]. When oxygen becomes limiting, levels of the HIF-1α subunit rise, enabling its dimerization with the HIF-β subunit. α,β-HIF activates gene expression that works to alleviate the effect of hypoxia in a context dependent manner [5]. HIF target genes, e.g. vascular endothelial growth factor (VEGF), are upregulated in many tumors, hence inhibition of HIF activity is a potential anti-cancer strategy [6–8]. The factors that regulates HIF target gene expression are still emerging, but it is clear that the transcriptional coactivator proteins p300/CREB (cAMP response element-binding protein)-binding protein (CBP) promote transcription of most, possibly all, HIF target genes [9,10]. Hence blocking the HIF-1α/p300 (CBP) interactions is of most interest as an anticancer target [11,12].

The HIF-1α/p300 protein–protein interaction (PPI) is tight ($K_D \approx 7$ nM) [13], involving the *C*-terminal transactivation domain (C-TAD) of HIF-1α/-2α isoforms binding to the CH1 (Cysteine/Histidine-rich 1) domain of p300/CBP (Fig. 1) [14–16]. Large surface interactions, as are observed between the HIF-1α C-TADs and p300/CBP, represent one of the challenges in inhibiting PPIs [17,18]. Interruption of the HIF-1α/p300 (CBP) interaction has been shown to negatively regulate oncogene expression and tumor growth [19–22]. Thus, the therapeutic significance of the HIF system has stimulated further high-throughput- and natural product-screening approaches for its inhibition [23–31]. The screens have employed both cell-based and isolated protein approaches; the cell-based approaches have yielded compounds that act indirectly on HIF, affecting the stability of HIF system proteins or by binding the hypoxia response elements (HREs) in DNA. Disrupting binding of HIF-1α to HREs has been demonstrated [25,32,33], though selectivity of DNA binders remains a concern.

In pioneering work, Kung et al. used a competition ELISA assay, with a biotinylated HIF-1α C-TAD truncate (785–826) and a GST-tagged CH1-domain, to identify chetomin, one of the epidithiodiketopiperazine (ETP) class of natural products, as a HIF-1α/

* Corresponding authors.
E-mail addresses: sam.thompson@chem.ox.ac.uk (S. Thompson), figgw@helix.nih.gov (W.D. Figg), andrew.hamilton@admin.ox.ac.uk (A.D. Hamilton).

http://dx.doi.org/10.1016/j.ejmech.2014.06.006
0223-5234/

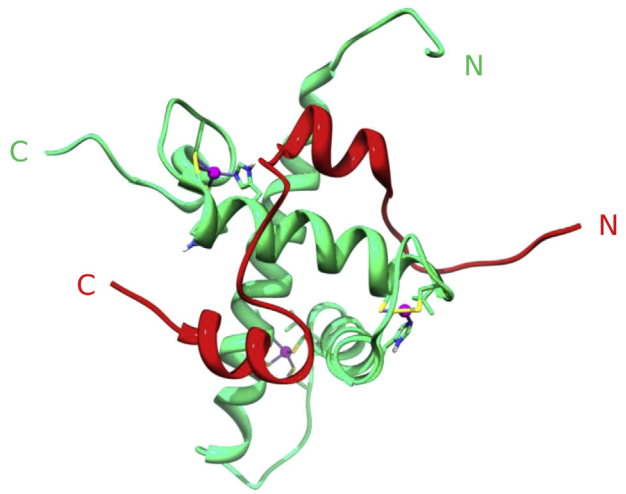

Fig. 1. View from an NMR structure of a fragment of the HIF-1α *C*-terminal transactivation domain (C-TAD) (785–826) (red) complexed with the CH1 domain of p300 (323–423) (green) with structurally important p300 zinc ions shown in magenta (PDB: IL3E) [14]. (For interpretation of the references to colour in this figure legend, the reader is referred to the web version of this article.)

p300 inhibitor [34]. The core, electrophilic, ETP functionality has been shown to be sufficient for activity, with a number of analogues showing similar activity to the natural products [35–37]. Subsequent work determined that chetomin and other ETPs work, at least in part, by Zn(II) ejection from the CH1 domain of p300, thus disrupting its structure, ablating the interaction with HIF-1α [38]. Modes of action involving cysteine modification and/or zinc ejection are likely inherently unselective, with the ETPs, such as chaetocin, showing inhibition against thioredoxin reductase and a number of histone methyl transferases [39–41].

In a search for inhibitors for the HIF-1α/p300 interaction we conducted an HTS of 10,000 natural product-based structures using a similar ELISA competition assay (Fig. 2). The results led to the identification of electrophilic inhibitors of the HIF-1α/p300 PPI.

2. Results and discussion

The output of the screen led to the identification of two distinct compound classes that showed promising activity: benzoquinones

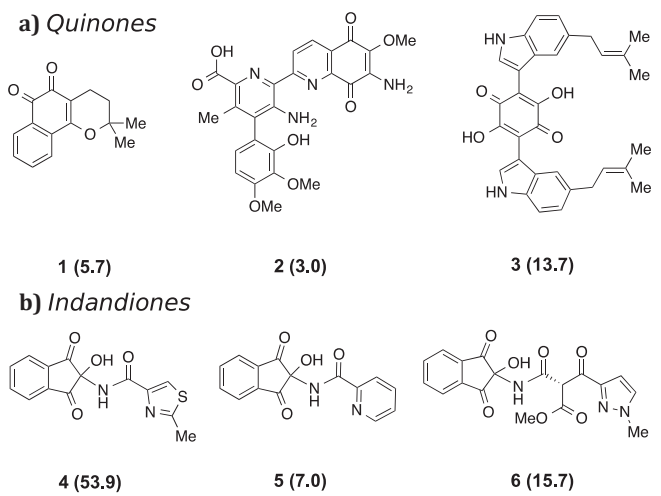

Fig. 2. Inhibitors of the HIF-1α/p300 interaction identified in a natural product-like compound screen. IC_{50} values (μM) are in parentheses; (a) benzoquinones; (b) indandiones.

1–**3**, and 2,2-disubstituted indandiones **4**–**6** (Fig. 2). The observation that a structurally diverse set of quinone derivatives displayed similar levels of activity suggested that the core quinone may be the active component. Indeed, we found that simple commercially available quinones were also active (Fig. 3). The results showed that the benzoquinone core is sufficient for activity, with potency correlating well with reported oxidative potentials [42,43]. Thus, anthraquinone **7** (half wave potential ($E_{1/2}$) = −1.26 V) was much less active than naphthoquinone **8** ($E_{1/2}$ = −1.03 V) or 2,3-dichloro-5,6-dicyano-1,4-benzoquinone (DDQ) **9** ($E_{1/2}$ = −0.34 V) [44,45].

Dipyridyldisulfide **13**, which contains a disulfide, as do the ETP inhibitors, was also weakly active (IC_{50} ≈ 100 μM). Analogous aromatic compounds, which did not contain quinone functionality, displayed no activity (e.g. **8** compared to **11**) although hydroquinones **10** and **12** showed modest activity. Hydroquinones may also be involved in a redox process, generating reactive quinones *in situ*. Spontaneous oxidation of hydroquinone and catechol by molecular oxygen has been observed to covalently modify DNA, suggesting that such redox cycles may be responsible for activity in our assay [46,47]. A common feature of the active compounds is the presence of electrophilic groups able to react with cysteines/thiols [48,49].

We then investigated the nature of the indandione-mediated inhibition. A range of 2-amino-, 2-imino- and 2-amidoindandiones **5**, **14**–**20** was synthesized to investigate SAR (Fig. 4a). The amino- and imino-derivatives **18**–**20** were less active than amido-derivatives **5** and **14**–**17** (Fig. 4b). Notably, ninhydrin **23** the parent compound of the indandione derivatives, displayed similar potency to the amido-derivatives (Fig. 4b, Supp. Info – Table S1), suggesting that ninhydrin may be the active component of the indandione compound class. Indeed, mass spectrometric and NMR analysis indicated that an aqueous solution of amido-compound **5** generates ninhydrin **23** (Fig. 5a). The decay of **5** to picolinamide and **23** was monitored by ^{1}H NMR at pH 8 (D_2O, 10 mM phosphate buffer), indicating that 80% hydrolysis occurs after one hour (Fig. 5b). Compounds that are structurally similar, but lack the reactive C-2 centre; i.e. 2-amido-indoline **21** and indandione **22**, were inactive (Fig. 4b). We thus propose that of all the apparently active indandione derivatives fragment to give ninhydrin **23**, which is the active species.

To further investigate the mode of action of these electrophilic compounds we tested whether they caused Zn(II) ejection from jumonji domain 2A histone demethylase (KDM4A), for which treatment with other Zn(II) ejectors has been shown to be inhibitory [50–52]. In the catalytic domain of KDM4A a Zn(II) ion is bound to three cysteines and one histidine in an analogous fashion to the coordination observed in the CH1 domain of p300 (Fig. 6b and c). Ebselen, a known zinc-ejector for KDM4A was used as a positive control, with the dye FluoZin-3™ (FZ-3) providing a measure of the unbound zinc concentration [50]. Compounds **8**, **10**, **16** and ninhydrin **23**, which were active in the competition binding assay also caused loss of Zn(II) from KDM4A in a dose and time dependent manner (Fig. 7b). Despite being less effective than ninhydrin **23** in the competition-binding assay, quinone **8** and reduced quinone **10** showed comparable KDM4A activity to **23**. Analogous studies on p300 yielded similar results, although the high basal levels of Zn(II), added to p300 such that it folds correctly, results in poorer resolution (Fig. 7a, Supp. Info – Fig. S2). The lack of selectivity observed by the quinones and indandiones identified in our initial screen suggest that they are likely not selective for different zinc binding sites [53,54].

When **8** and **23** were tested in a HeLa cell viability assay, significant dose-dependent cytotoxicity was observed after 48 h (Supp. Info – Fig. S3). The inactive compound **21** was not cytotoxic

Please cite this article in press as: M.K.P. Jayatunga, et al., Inhibition of the HIF1α-p300 interaction by quinone- and indandione-mediated ejection of structural Zn(II), European Journal of Medicinal Chemistry (2014), http://dx.doi.org/10.1016/j.ejmech.2014.06.006

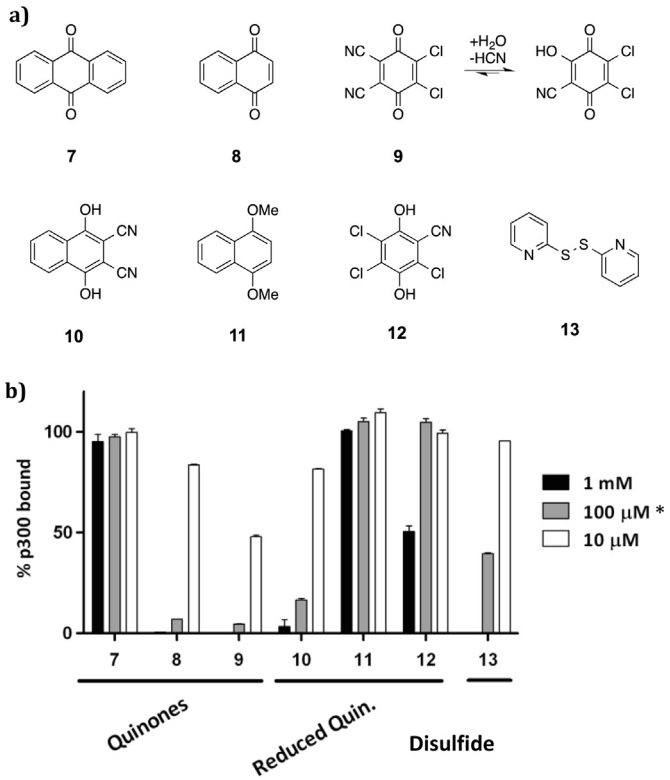

Fig. 3. Assays of commericially available quinones **7**–**12** and disulfide **13** for disrupting the HIF-1α (785–826)/p300 CH1 domain (323–423) binding. (a) tested compounds; (b) assay results (1% DMSO; triplicate, ±SD). *__7__, __9__, __10__, __13__ were tested at 100 μM, __8__, __11__, __12__ were tested at 63 μM.

under the tested conditions. Naphthoquinone **8**, ninhydrin **23** and related compounds have been shown to form protein adducts resulting in nonspecific toxicity [55,56].

3. Conclusions

In conclusion, our results have validated the output of an HTS on the HIF-1α/p300 interaction which led to the identification of quinone and indandione inhibitors. Subsequent studies demonstrated that the core quinone and ninhydrin parent rings are sufficient for inhibition, which likely occurs via non-selective loss of zinc ions, leading to disruption of the domain fold. Whilst it is possible that appropriate derivatisation could enable selectivity to be achieved, the available evidence is that this will be non-trivial. Further, we note that related electrophilic and redox sensitive compounds have also been shown to inhibit the hypoxia system (Table 1). ETPs have been shown to have targets other than p300, including histone methyl transferases (HKMTs) and thioredoxin reductase (TrxR), where reaction with thiols is also proposed [34,40,41]. A variety of quinone containing compounds have also been suggested to inhibit HIF-1α either directly [29,31] or indirectly by interacting with HIF-1α stabilizing proteins [30,57–60]. The prevalence of potentially reactive inhibitors against p300, and hypoxia system proteins thioredoxin (Trx) and TrxR, might indicate that proteins involved in this cascade are particularly sensitive to electrophilic molecules.

Whether the repeated identification of redox sensitive compounds in screens on the hypoxia system/HIF components is more than coincidence is unknown at this stage. However, the development of such compounds into (selective) pharmaceuticals could be problematic, and it may be of interest to configure (at least some of) the outputs of future screens to indentify such compounds [61,62].

4. Experimental

4.1. General information

Reactions were carried out under a nitrogen or argon atmosphere in oven-dried glassware at room temperature unless otherwise stated. Standard inert atmosphere techniques were used in handling all air and moisture sensitive reagents.

Anhydrous acetonitrile and dichloromethane (from commercial sources) were obtained by filtration through activated alumina (powder ~ 150 mesh, pore size 58 Å, basic, Sigma–Aldrich) columns, or were dried on an MB-SPS-800 dry solvent system. Other solvents and reagents were used directly as received from commercial suppliers. Petrol refers to distilled light petroleum of fraction (30 °C–40 °C).

Flash column chromatography was carried out using VWR Kieselgel 60 silica gel (60–63 μm). Thin-layer chromatography was carried out using Merck Kieselgel 60 F254 (230–400 mesh) fluorescent treated silica, visualized under UV light (250 nm) and by staining with aqueous potassium permanganate solution.

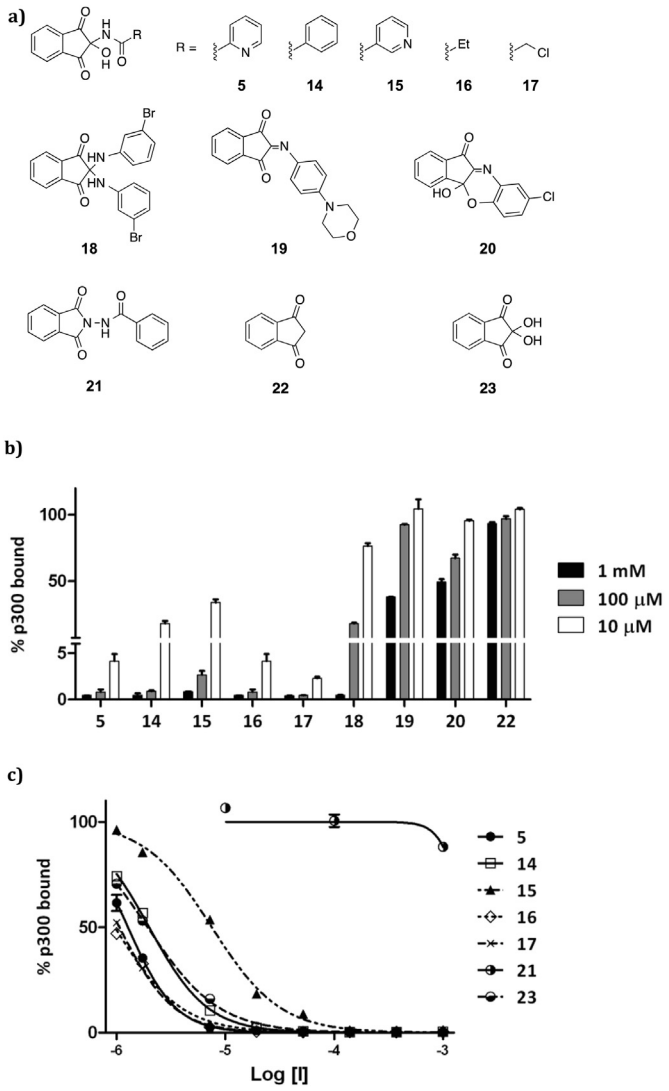

Fig. 4. Assays with ninhydrin related compounds (a) tested compounds included mono- (**5**, **14**–**17**) and di-substituted ninhydrin adducts (**18**) and related derivatives (**19**–**22**); (b) Inhibition data of tested compounds at three doses; (c) dose response curves for selected compounds (**5**, **14**–**17**, **21** and **23**; 1% DMSO; triplicate, ±SD).

Please cite this article in press as: M.K.P. Jayatunga, et al., Inhibition of the HIF1α-p300 interaction by quinone- and indandione-mediated ejection of structural Zn(II), European Journal of Medicinal Chemistry (2014), http://dx.doi.org/10.1016/j.ejmech.2014.06.006

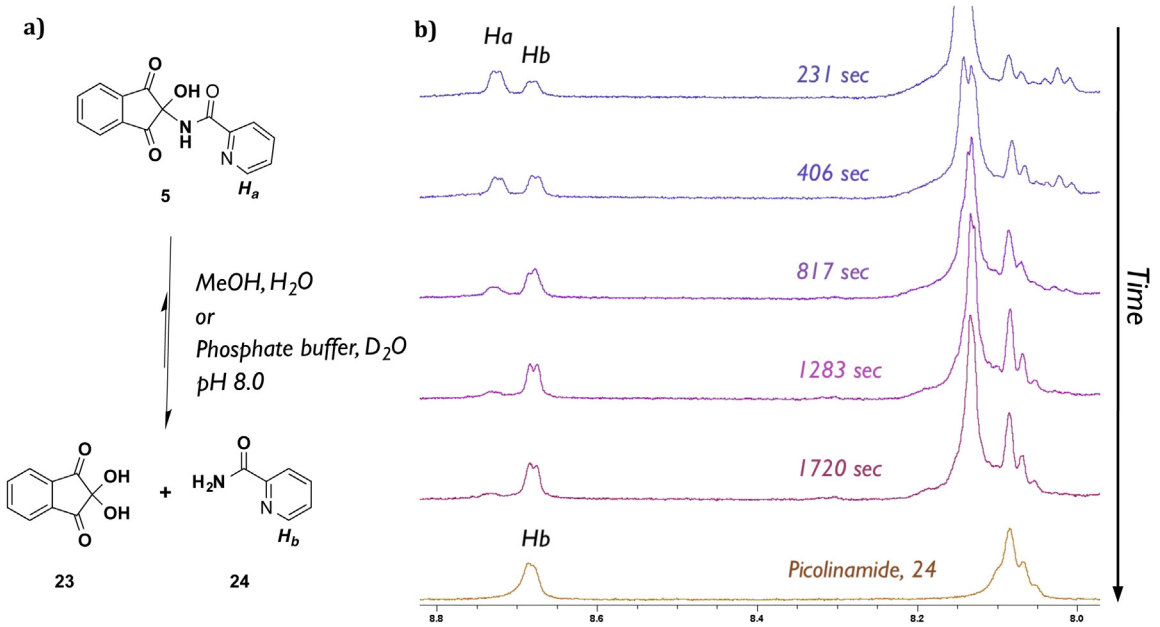

Fig. 5. The ninhydrin adducts undergo fragmentation in aqueous solution. Adduct **5** was dissolved in deuterated phosphate buffer (pH 8) and its stability was monitored by ^{1}H NMR (500 MHz), with increased Increased appearance of picolinamide **24** signal Hb consistent with fragmentation.

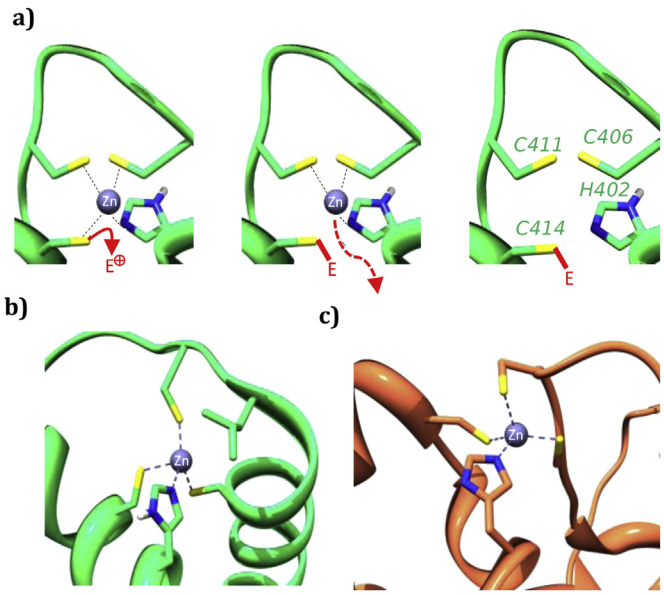

Fig. 6. Proposed outline mechanism of electrophile-promoted Zn(II) ejection from p300 (a); Zn(II) binding sites in the CH1 domain of p300 (b) are structurally similar to those found in other proteins including the catalytic domain of KDM4A (c). PDB: p300: IL3E and KDM4A: 2PXJ respectively [14,52].

^{1}H and ^{13}C NMR spectra were recorded using a Bruker 500, 400 or 300 MHz spectrometer running Topspin™ software and are quoted in ppm for measurement against a residual solvent peak as an internal standard. Chemical shifts (δ) are given in parts per million (ppm), and coupling constants (J) are given in Hertz (Hz). The ^{1}H NMR spectra are reported as follows: δ/ppm (number of protons, multiplicity, coupling constant J/Hz (where appropriate), assignment). Multiplicity is abbreviated as follows: s = singlet, br = broad, d = doublet, dd = doublet of doublets, t = triplet, dt = doublet of triplet, q = quartet, dq = doublet of quartet, qn = quintet, sept = septet, m = multiplet. Compound names are those generated by ChemBioDraw™ (CambridgeSoft) following IUPAC nomenclature. However, the NMR assignment numbering used is arbitrary and does not follow any particular convention. Numbering of compounds is illustrated on the spectra themselves; *vide infra*. The ^{13}C NMR spectra are reported in δ/ppm. Two-dimensional (COSY, HSQC, HMBC) NMR spectroscopy was used to assist the assignment of signals in the ^{1}H and ^{13}C NMR spectra. IR spectra were recorded on a Bruker Tensor 27 FT-IR spectrometer from a thin film deposited onto a diamond ATR module. Only selected maximum absorbances (ν_{max}) of the most intense peaks are reported (cm^{-1}). High-resolution mass spectra were recorded on a Bruker MicroTof mass spectrometer (ESI) by the internal service at the Department of Organic Chemistry, University of Oxford. Melting points were recorded using a Leica Galen III hot-stage microscope apparatus and are reported uncorrected in Celsius (°C).

4.1.1. *N-(2-hydroxy-1,3-dioxo-2,3-dihydro-1H-inden-2-yl) picolinamide (**5**)*

Ninhydrin (400 mg, 2.25 mmol) and picolinamide (274 mg, 2.25 mmol) were added to a mixture of acetonitrile (15 mL) and anhydrous $MgSO_4$ (150 mg) and the mixture was stirred at room temperature for 2 h. The mixture was filtered and washed with acetonitrile (15 mL). The solvent was removed from the filtrate *in vacuo* and the resulting residue was dissolved in dichloromethane (50 mL). The resulting solution was partitioned with water (50 mL). The product was crystallized from the aqueous phase as pale green crystals (27 mg, 0.10 mmol, 4%); m.p. 163–164; δ_H (400 MHz, d_6-DMSO): 9.10 (1H, s); 8.73 (1H, d, J 4.7); 8.10–8.03 (5H, m); 8.00 (1H, td, J 1.6, 7.7); 7.84 (1H, d, J 7.8); 7.68 (1H, ddd, J 1.1, 4.8, 7.6); δ_C (100 MHz, d_6-DMSO): 196.0; 163.6; 149.0; 147.6; 138.6; 138.1; 137.0; 127.5; 123.7; 121.9; 79.7; IR ν_{max}: 3291, 3020, 1748, 1710, 1657, 1360, 1096, 960, 736: HRMS (ESI) found 305.0529; $C_{15}H_{10}N_2NaO_4$ $[M+Na]^+$ requires 305.0533.

4.1.2. *N-(2-hydroxy-1,3-dioxo-2,3-dihydro-1H-inden-2-yl) benzamide (**14**)*

Ninhydrin (500 mg, 2.81 mmol) and benzamide (340 mg, 2.81 mmol) were added to a mixture of acetonitrile (15 mL) and

Please cite this article in press as: M.K.P. Jayatunga, et al., Inhibition of the HIF1α-p300 interaction by quinone- and indandione-mediated ejection of structural Zn(II), European Journal of Medicinal Chemistry (2014), http://dx.doi.org/10.1016/j.ejmech.2014.06.006

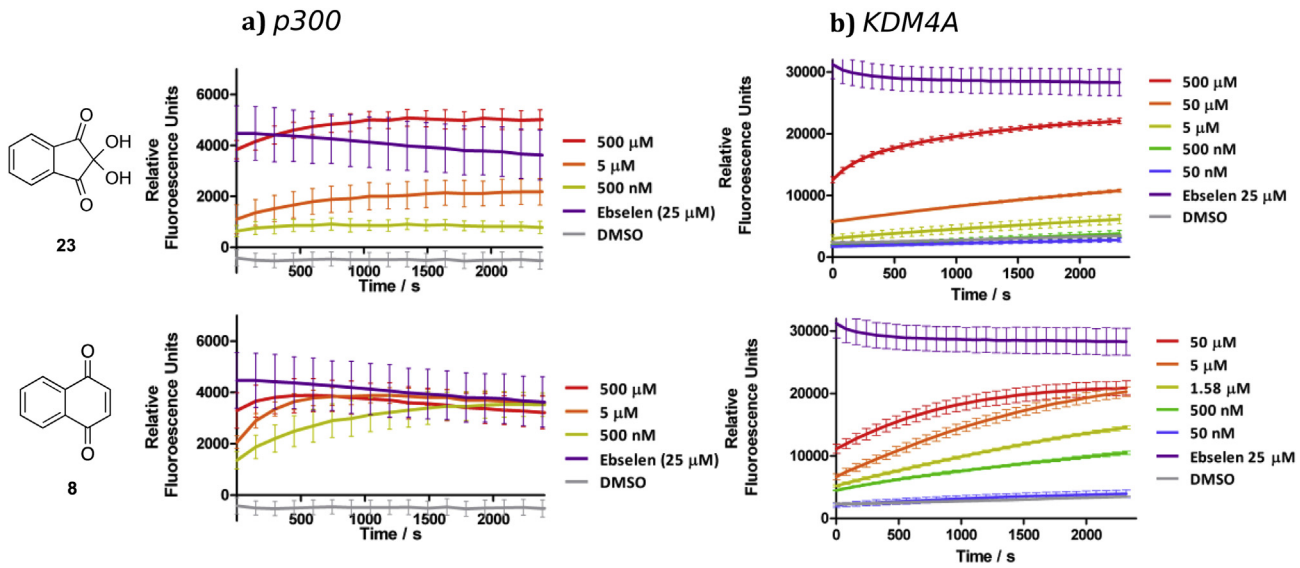

Fig. 7. Zinc ejector behavior of ninhydrin **23**, and benzoquinone **8** against a) p300 and b) KDM4A. Fluorescence-based assays for release of Zn(II) from the CH1 domain of p300 and the catalytic domain of KDM4A. Compounds show a dose- and time-dependent increase in fluorescence as Zn(II) is released into the buffer. Established zinc ejector ebselen was used as a positive control for Zn(II) release.

anhydrous $MgSO_4$ (150 mg) and the mixture was stirred at room temperature for 2 h. The mixture was filtered and washed with acetonitrile (15 mL). The solvent was removed from the filtrate *in vacuo* and the resulting residue was dissolved in dichloromethane (50 mL). The resulting solution was partitioned with water (50 mL). The aqueous phase was washed with dichloromethane (3 × 50 mL). The solvent was removed from the combined organic phase *in vacuo* to yield the product as a white solid (264 mg, 0.93 mmol, 34%); m.p. 125–126; δ_H (400 MHz, d_6-DMSO): 9.82 (1H, s); 8.07–8.00 (4H, m); 7.96 (1H, s); 7.93–7.85 (2H, m); 7.58–7.42 (3H, m); δ_C (100 MHz, d_6-DMSO): 197.31; 166.9; 139.2; 137.5; 133.0; 132.1; 129.1; 128.7; 124.5; 81.4; IR ν_{max}: 3274, 1719, 1645, 1270, 1195, 1120, 967, 736. HRMS (ESI) found 304.0583; $C_{16}H_{11}NNaO_4$ $[M+Na]^+$ requires 304.0580.

4.1.3. N-(2-hydroxy-1,3-dioxo-2,3-dihydro-1H-inden-2-yl) propionamide (**15**)

The *title* compound (**15**) was prepared from ninhydrin (500 mg, 2.81 mmol) and propionamide (204 mg, 2.81 mmol) by following a procedure analogous to the one used for the synthesis of **14**. The product was isolated as a cream solid (390 mg, 1.67 mmol, 60%); m.p. 153–154; δ_H (400 MHz, d_6-DMSO): 9.14 (1H, s); 8.03–7.95 (4H, m); 7.69 (1H, s); 2.13 (2H, q, *J* 7.6); 0.87 (3H, t, *J* 7.6); δ_C (100 MHz, d_6-DMSO): 197.7; 174.0; 139.3; 137.4; 124.3; 80.2; 27.4; 10.1; IR ν_{max}: 3375, 3133 (br), 1760, 1723, 1632, 1513, 1116, 965, 737. HRMS (ESI) found 256.0581; $C_{12}H_{11}NNaO_4$ $[M+Na]^+$ requires 256.0580.

4.1.4. N-(2-hydroxy-1,3-dioxo-2,3-dihydro-1H-inden-2-yl) nicotinamide (**16**)

Ninhydrin (500 mg, 2.81 mmol) and nicotinamide (342 mg, 2.81 mmol) were added to a mixture of acetonitrile (15 mL) and anhydrous $MgSO_4$ (150 mg) and the mixture was stirred at room temperature for 2 h. The mixture was filtered, washed with acetonitrile, concentrated and the resulting residue was dissolved in dichloromethane (50 mL). The resulting solution was partitioned with water (50 mL). The product was crystallized from the aqueous phase as pale green crystals (43 mg, 0.15 mmol, 5%); m.p. 199; δ_H (500 MHz, d_6-DMSO): 10.10 (1H, s); 9.04 (1H, d, *J* 1.7); 8.74 (1H, dd, *J* 1.6, 4.8); 8.24 (1H, dt, *J* 2.0, 8.0); 8.09–8.00 (5H, m); 7.51 (1H, dd, *J* 4.7, 7.8); δ_C (500 MHz, d_6-DMSO): 196.2; 164.6; 152.7; 148.9; 138.4; 136.5; 135.5; 126.7; 123.7; 123.4; 80.6; IR ν_{max}: 3344, 3270, 2980, 2696, 1753, 1716, 1191, 1124, 736. HRMS (ESI) found 305.0540; $C_{15}H_{10}N_2NaO_4$ $[M+Na]^+$ requires 305.0533.

4.1.5. 2-Chloro-N-(2-hydroxy-1,3-dioxo-2,3-dihydro-1H-inden-2-yl)acetamide (**17**)

Ninhydrin (500 mg, 2.81 mmol) and 2-chloroacetamide (260 mg, 2.81 mmol) were added to a mixture of acetonitrile (15 mL) and anhydrous $MgSO_4$ (150 mg) and the mixture was stirred at room temperature for 2 h. The mixture was filtered, washed with acetonitrile, concentrated and the resulting residue dissolved in dichloromethane (50 mL). The resulting solution was partitioned with water (50 mL). The aqueous phase was washed with dichloromethane (3 × 50 mL). The solvent was removed from the combined organic phase *in vacuo*, and the residue was washed with ether to yield the product as a pink solid (31 mg, 0.12 mmol, 4%); m.p. 140–143; δ_H (400 MHz, d_6-DMSO): 9.61 (1H, s); 8.07–7.98 (4H, m); 7.96 (1H, s); 4.10 (2H, s); δ_C (100 MHz, d_6-DMSO): 196.8; 166.7; 139.3; 137.8; 124.5; 80.4; 41.8; IR ν_{max}: 3364, 3157 (br), 2942, 1760, 1660, 1468, 1353, 1117, 740, 696. HRMS (ESI) found 276.0035; $C_{11}H_8^{35}ClNNaO_4$ $[M+Na]^+$ requires 276.0034.

4.1.6. 2,2-Bis((3-bromophenyl)amino)-1H-indene-1,3(2H)-dione (**18**)

According to literature procedure [63], 3-bromoaniline (0.28 mL, 2.66 mmol) was added to a solution of ninhydrin (473 mg, 2.66 mmol) in water (5.0 mL). After stirring at room temperature for 1 h, the yellow precipitate was filtered and washed with cold water. The residue was recrystalised from hexane:chloroform (1:5) to give the *title compound* **18** as a red/brown crystalline solid (150 mg, 0.31 mmol, 12%), m.p.. 142–143; δ_H (400 MHz, d_6-DMSO): 8.71 (4H, m); 7.23 (2H, t, *J* 1.8); 7.13 (2H, s); 6.97 (2H, t, *J* 8.0); 6.83 (2H, dd, *J* 1.5, 8.2); 6.79 (2H, dd, *J* 0.9, 7.8); δ_C (100 MHz, d_6-DMSO): 194.9; 147.2; 139.0; 138.3; 131.1; 125.2; 122.5; 121.5; 118.5; 115.0; 73.8; IR ν_{max}: 3377, 1696, 1589, 1474, 1256, 1138, 961, 767. HRMS (ESI) found 484.9332; $C_{21}H_{14}^{79}Br_2N_2O_2$ $[M+H]^+$ requires 494.9330.

Please cite this article in press as: M.K.P. Jayatunga, et al., Inhibition of the HIF1α-p300 interaction by quinone- and indandione-mediated ejection of structural Zn(II), European Journal of Medicinal Chemistry (2014), http://dx.doi.org/10.1016/j.ejmech.2014.06.006

Table 1
Literature inhibitors of the HIF system and HIF system components. Potentially electrophilic functionality is shown in bold.

Inhibitor	Reported target (proposed)	Reference
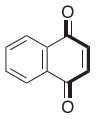 **8**	HIF-1α/p300 KDM4A Others	[55]
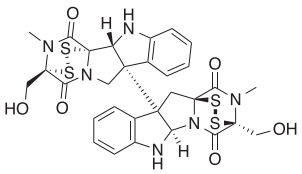 **25, Chaetocin**	HIF-1α/p300 HKMTs TrxR	[34,40–42]
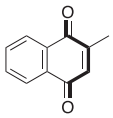 **26**	HIF-1α/p300	[29]
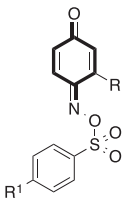 **27**	HIF-1α/p300	[31]
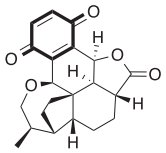 **28, Pleurotin**	Trx-1 (indirectly on HIF-1α)	[30]
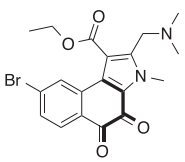 **29**	HIF-1α/p300	[57]
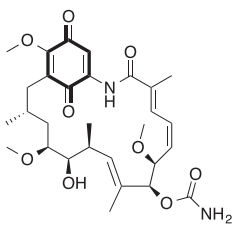 **30, Geldanamycin**	HSP90 (indirectly on HIF-1α)	[58,59]

4.1.7. 2-((4-Morpholinophenyl)imino)-1H-indene-1,3(2H)-dione (**19**)

A solution of ninhydrin (662 mg, 3.71 mmol) in water (10 mL) was added dropwise to a suspension of 4-morpholinoaniline (662 mg, 3.71 mmol) in water (10 mL). After stirring for 1 h, the brown precipitate was filtered and washed with MeOH (15 mL). The residue was recrystalised from MeOH to give the *title compound* **19** as dark purple crystals. (215 mg, 0.67 mmol, 18%); m.p. 212–214; δ_H (400 MHz, d_6-DMSO): 7.99–7.94 (4H, m); 7.77 (2H, d, *J* 9.2); 7.03 (2H, d, *J* 9.2); 3.8 (2H, t, *J* 5.0); 3.40 (2H, t, *J* 5.0). δ_C (100 MHz, d_6-DMSO): 188.0; 153.3; 140.9; 138.3; 136.9; 136.8; 130.7; 124.5; 113.8; 66.7; 47.7; IR ν_{max}: 1716, 1675, 1483, 1160, 1114, 979, 827; HRMS (ESI) found 343.1042; $C_{19}H_{16}N_2NaO_2$ $[M+Na]^+$ requires 343.1053.

4.1.8. (±)8-Chloro-4b-hydroxybenzo[b]indeno[2,1-e][1,4]oxazin-11(4bH)-one (**20**)

A solution of ninhydrin (1.48 g, 8.31 mmol) in water (20 mL) was added to a solution of 2-amino-4-chlorophenol (1.19 g, 8.31 mmol) in water (10 mL). A few drops of pyridine were added and the mixture was stirred for 1 h. The precipitate was filtered and concentrated *in vacuo* affording the crude product as a white solid (2.08 g). A 500 mg sample of the residue was recrystalised from MeOH to give the *title compound* **20** as yellow/green crystals (40 mg, 0.14 mmol, 2%); m.p. 273–275; δ_H (500 MHz, d_6-DMSO): 8.70 (1H, s); 8.19 (1H, d, *J* 7.8); 8.05–8.01 (2H, m); 7.90 (1H, t, *J* 7.7); 7.68 (1H, d, *J* 2.6); 7.38 (1H, dd, *J* 2.5, 8.7); 7.30 (1H, d, *J* 8.7); δ_C (125 MHz, d_6-DMSO): 191.6; 159.4; 143.8; 141.1; 137.5; 136.1; 134.9; 134.44; 128.4; 126.8; 126.7; 124.9; 123.9; 119.6; 86.0; IR ν_{max}: 2862, 1740, 1675, 1440, 1217, 971, 826, 717. HRMS (ESI) found 285.0215; $C_{15}H_8^{(35)}ClNO_3$ $[M+H]^+$ requires 285.0193.

4.1.9. N-(1,3-dioxoisoindolin-2-yl)benzamide (**21**)

According to literature procedure [64], phthalic anhydride (500 mg, 3.37 mmol) and benzohydrazine (545 mg, 4.00 mmol) were added to acetic acid (20 mL) and the mixture was heated at 125 °C for 2 h. The reaction was cooled to room temperature and water (35 mL, kept at 0 °C) was added. The white precipitate was filtered, washed with cold water and concentrated *in vacuo* to give the *title compound* **21** (517 mg, 1.9 mmol, 57%); m.p. 214–215; δ_H (400 MHz, d_6-DMSO): 11.34 (1H, s); 8.04–7.96 (6H, m); 7.68 (1H, t, *J* 7.7); 7.58 (2H, t, *J* 7.7); δ_C (100 MHz, d_6-DMSO): 165.37; 165.38; 135.5; 132.8; 130.7; 129.5; 128.8; 127.8; 123.90; IR ν_{max}: 3232 (br), 1799, 1733, 1662, 1282, 1118, 878, 700. HRMS (ESI) found 265.0617; $C_{15}H_9N_2O_4$ $[M-H]^-$ requires 265.0619.

Acknowledgments

We thank Cancer Research UK (MKPJ), the Wellcome Trust, and the University of Oxford (ST) for funding. This work was supported in part by the Intramural Research Program of the National Institutes of Health, National Cancer Institute, Bethesda, MD, USA.

Appendix A. Supplementary data

Supplementary data related to this article can be found at http://dx.doi.org/10.1016/j.ejmech.2014.06.006.

References

[1] R.J. Gillies, R.A. Gatenby, Hypoxia and adaptive landscapes in the evolution of carcinogenesis, Cancer Metastasis Rev. 26 (2007) 311–317.
[2] N.V. Iyer, L.E. Kotch, F. Agani, S.W. Leung, E. Laughner, R.H. Wenger, et al., Cellular and developmental control of O_2 homeostasis by hypoxia-inducible factor 1α, Genes. Dev. 12 (1998) 149–162.

[3] E.K. Rofstad, T. Danielsen, Hypoxia-induced angiogenesis and vascular endothelial growth factor secretion in human melanoma, Br. J. Cancer 77 (1998) 897–902.
[4] S.D. Young, R.S. Marshall, R.P. Hill, Hypoxia induces DNA overreplication and enhances metastatic potential of murine tumor cells, Proc. Natl. Acad. Sci. U. S. A. 85 (1988) 9533–9537.
[5] G.L. Wang, B.H. Jiang, E.A. Rue, G.L. Semenza, Hypoxia-inducible factor 1 is a basic-helix-loop-helix-PAS heterodimer regulated by cellular O_2 tension, Proc. Natl. Acad. Sci. U. S. A. 92 (1995) 5510–5514.
[6] Y. Baba, K. Nosho, K. Shima, N. Irahara, A.T. Chan, J.A. Meyerhardt, et al., HIF-1α overexpression is associated with poor prognosis in a cohort of 731 colorectal cancers, Am. J. Pathol. 176 (2010) 2292–2301.
[7] N. Akakura, M. Kobayashi, I. Horiuchi, A. Suzuki, J. Wang, J. Chen, et al., Constitutive expression of hypoxia-inducible factor-1α renders pancreatic cancer cells resistant to apoptosis induced by hypoxia and nutrient deprivation, Cancer Res. 61 (2001) 6548–6554.
[8] H. Zhong, A.M.D. Marzo, E. Laughner, M. Lim, D.A. Hilton, D. Zagzag, et al., Overexpression of hypoxia-inducible factor-1α in common human cancers and their metastases, Cancer Res. 59 (1999) 5830–5835.
[9] Z. Arany, L.E. Huang, R. Eckner, S. Bhattacharya, C. Jiang, M.A. Goldberg, et al., An essential role for p300/CBP in the cellular response to hypoxia, Proc. Natl. Acad. Sci. U. S. A. 93 (1996) 12969–12973.
[10] B.H. Jiang, E. Rue, G.L. Wang, R. Roe, G.L. Semenza, Dimerization, DNA binding, and transactivation properties of hypoxia-inducible factor 1, J. Biol. Chem. 271 (1996) 17771–17778.
[11] A. Giaccia, B.G. Siim, R.S. Johnson, HIF-1 as a target for drug development, Nat. Rev. Drug. Discov. 2 (2003) 803–811.
[12] G.L. Semenza, Targeting HIF-1 for cancer therapy, Nat. Rev. Cancer 3 (2003) 721–732.
[13] G.L. Semenza, Physiology meets biophysics: visualizing the interaction of hypoxia-inducible factor-1α with p300 and CBP, Proc. Natl. Acad. Sci. U. S. A. 99 (2002) 11570–11572.
[14] S.J. Freedman, Z.-Y.J. Sun, F. Poy, A.L. Kung, D.M. Livingston, G. Wagner, et al., Structural basis for recruitment of CBP/p300 by hypoxia-inducible factor-1α, Proc. Natl. Acad. Sci. U. S. A. 99 (2002) 5367–5372.
[15] J. Gu, J. Milligan, L.E. Huang, Molecular mechanism of hypoxia-inducible factor 1alpha-p300 interaction. A leucine-rich interface regulated by a single cysteine, J. Biol. Chem. 276 (2001) 3550–3554.
[16] A.L. Kung, S. Wang, J.M. Klco, W.G. Kaelin, D.M. Livingston, Suppression of tumor growth through disruption of hypoxia-inducible transcription, Nat. Med. 6 (2000) 1335–1340.
[17] W.E. Stites, Protein–protein interactions: interface structure, binding thermodynamics, and mutational analysis, Chem. Rev. 97 (1997) 1233–1250.
[18] S. Jones, J.M. Thornton, Principles of protein-protein interactions, Proc. Natl. Acad. Sci. U. S. A. 93 (1996) 13–20.
[19] L.K. Henchey, S. Kushal, R. Dubey, R.N. Chapman, B.Z. Olenyuk, P.S. Arora, Inhibition of hypoxia inducible factor 1—transcription coactivator interaction by a hydrogen bond surrogate α-Helix, J. Am. Chem. Soc. 132 (2010) 941–943.
[20] S. Kushal, B.B. Lao, L.K. Henchey, R. Dubey, H. Mesallati, N.J. Traaseth, et al., Protein domain mimetics as in vivo modulators of hypoxia-inducible factor signaling, Proc. Natl. Acad. Sci. U. S. A. (2013) 15602–15607.
[21] G.M. Burslem, H.F. Kyle, A.L. Breeze, T.A. Edwards, A. Nelson, S.L. Warriner, et al., Small-molecule proteomimetic inhibitors of the HIF-1α–p300 protein–-protein interaction, ChemBioChem (2014) 1083–1087.
[22] B.B. Lao, I. Grishagin, H. Mesallati, T.F. Brewer, B.Z. Olenyuk, P.S. Arora, In vivo modulation of hypoxia-inducible signaling by topographical helix mimetics, Proc. Natl. Acad. Sci. U. S. A. (2014) 7531–7536.
[23] W. Huang, R. Huang, M.S. Attene-Ramos, S. Sakamuru, E.E. Englund, J. Inglese, et al., Synthesis and evaluation of quinazolin-4-ones as hypoxia-inducible factor-1α inhibitors, Bioorg. Med. Chem. Lett. 21 (2011) 5239–5243.
[24] V. Moreno-Manzano, F.J. Rodríguez-Jiménez, J.L. Aceña-Bonilla, S. Fustero-Lardíes, S. Erceg, J. Dopazo, et al., FM19G11, a new hypoxia-inducible factor (HIF) modulator, affects stem cell differentiation status, J. Biol. Chem. 285 (2010) 1333–1342.
[25] D. Kong, E.J. Park, A.G. Stephen, M. Calvani, J.H. Cardellina, A. Monks, et al., Echinomycin, a small-molecule inhibitor of hypoxia-inducible factor-1 DNA-binding activity, Cancer Res. 65 (2005) 9047–9055.
[26] C. Tan, R.G. de Noronha, A.J. Roecker, B. Pyrzynska, F. Khwaja, Z. Zhang, et al., Identification of a novel small-molecule inhibitor of the hypoxia-inducible factor 1 pathway, Cancer Res. 65 (2005) 605–612.
[27] K. Lee, J.H. Lee, S.K. Boovanahalli, Y. Jin, M. Lee, X. Jin, et al., (Aryloxyacetylamino)benzoic acid analogues: a new class of hypoxia-inducible factor-1 inhibitors, J. Med. Chem. 50 (2007) 1675–1684.
[28] H.S. Kwon, D.-R. Kim, E.G. Yang, Y.K. Park, H.-C. Ahn, S.-J. Min, et al., Inhibition of VEGF transcription through blockade of the hypoxia inducible factor-1α–p300 interaction by a small molecule, Bioorg. Med. Chem. Lett. 22 (2012) 5249–5252.
[29] Y.-R. Na, K.-C. Han, H. Park, E.G. Yang, Menadione and ethacrynic acid inhibit the hypoxia-inducible factor (HIF) pathway by disrupting HIF-1α interaction with p300, Biochem. Biophys. Res. Commun. 434 (2013) 879–884.
[30] S.J. Welsh, R.R. Williams, A. Birmingham, D.J. Newman, D.L. Kirkpatrick, G. Powis, The thioredoxin redox inhibitors 1-methylpropyl 2-imidazolyl disulfide and pleurotin inhibit hypoxia-induced factor 1α and vascular endothelial growth factor formation 1, Mol. Cancer Ther. 2 (2003) 235–243.
[31] H. Yang, C.E. Pinello, J. Luo, D. Li, Y. Wang, L.Y. Zhao, et al., Small-molecule inhibitors of acetyltransferase p300 identified by high-throughput screening are potent anticancer agents, Mol. Cancer Ther. 12 (2013) 610–620.
[32] B.Z. Olenyuk, G.-J. Zhang, J.M. Klco, N.G. Nickols, W.G. Kaelin, P.B. Dervan, Inhibition of vascular endothelial growth factor with a sequence-specific hypoxia response element antagonist, Proc. Natl. Acad. Sci. U. S. A. 101 (2004) 16768–16773.
[33] N.G. Nickols, C.S. Jacobs, M.E. Farkas, P.B. Dervan, Modulating hypoxia-inducible transcription by disrupting the HIF-1–DNA interface, ACS Chem. Biol. 2 (2007) 561–571.
[34] A.L. Kung, S.D. Zabludoff, D.S. France, S.J. Freedman, E.A. Tanner, A. Vieira, et al., Small molecule blockade of transcriptional coactivation of the hypoxia-inducible factor pathway, Cancer Cell 6 (2004) 33–43.
[35] K.M. Block, H. Wang, L.Z. Szabo, N.W. Polaske, L.K. Henchey, R. Dubey, et al., Direct inhibition of hypoxia-inducible transcription factor complex with designed dimeric epidithiodiketopiperazine, J. Am. Chem. Soc. 131 (2009) 18078–18088.
[36] R. Dubey, M.D. Levin, L.Z. Szabo, C.F. Laszlo, S. Kushal, J.B. Singh, et al., Suppression of tumor growth by designed dimeric epidithiodiketopiperazine targeting hypoxia-inducible transcription factor complex, J. Am. Chem. Soc. 135 (2013) 4537–4549.
[37] S. Kushal, H. Wang, C.F. László, L.Z. Szábo, B.Z. Olenyuk, Inhibition of hypoxia-inducible transcription factor complex with designed epipolythiodiketopiperazine, Biopolymers 95 (2011) 8–16.
[38] K.M. Cook, S.T. Hilton, J. Mecinovic, W.B. Motherwell, W.D. Figg, C.J. Schofield, Epidithiodiketopiperazines block the interaction between hypoxia-inducible factor-1alpha (HIF-1alpha) and p300 by a zinc ejection mechanism, J. Biol. Chem. 284 (2009) 26831–26838.
[39] F.L. Cherblanc, K.L. Chapman, R. Brown, M.J. Fuchter, Chaetocin is a nonspecific inhibitor of histone lysine methyltransferases, Nat. Chem. Biol. 9 (2013) 136–137.
[40] F.L. Cherblanc, K.L. Chapman, J. Reid, A.J. Borg, S. Sundriyal, L. Alcazar-Fuoli, et al., On the histone lysine methyltransferase activity of fungal metabolite chaetocin, J. Med. Chem. 56 (2013) 8616–8625.
[41] J.D. Tibodeau, L.M. Benson, C.R. Isham, W.G. Owen, K.C. Bible, The anticancer agent chaetocin is a competitive substrate and inhibitor of thioredoxin reductase, Antioxid. Redox Signal 11 (2009) 1097–1106.
[42] L. Klupfel, Redox Characteristics of Quinones in Natural Organic Matter (NOM), PhD term paper, ETH Zurich, 2009.
[43] A. Beheshti, P. Norouzi, M.R. Ganjali, A simple and robust model for predicting the reduction potential of quinones family; electrophilicity index effect, Int. J. Electrochem. Sci. (2012) 4811–4821.
[44] C. Frontana, Á. Vázquez-Mayagoitia, J. Garza, R. Vargas, I. González, Substituent effect on a family of quinones in aprotic solvents: an experimental and theoretical approach, J. Phys. Chem. A 110 (2006) 9411–9419.
[45] The half-wave potential for DDQ was not found in the study by Frontana. The value quoted is for the 2,3,5,6-tetrachloro-1,4-quinone which is expected to be similar to 2,3-dichloro-5,6-cyano-1,4-quinone., DDQ half wave potential.
[46] E. Sella, D. Shabat, Hydroquinone–quinone oxidation by molecular oxygen: a simple tool for signal amplification through auto-generation of hydrogen peroxide, Org. Biomol. Chem. 11 (2013) 5074–5078.
[47] K. Hirakawa, S. Oikawa, Y. Hiraku, I. Hirosawa, S. Kawanishi, Catechol and hydroquinone have different redox properties responsible for their differential DNA-damaging ability, Chem. Res. Toxicol. 15 (2002) 76–82.
[48] V. Ehmke, J.E.Q. Quinsaat, P. Rivera-Fuentes, C. Heindl, C. Freymond, M. Rottmann, et al., Tuning and predicting biological affinity: aryl nitriles as cysteine protease inhibitors, Org. Biomol. Chem. 10 (2012) 5764–5768.
[49] W.-W. Li, J. Heinze, W. Haehnel, Site-specific binding of quinones to proteins through thiol addition and addition-elimination reactions, J. Am. Chem. Soc. 127 (2005) 6140–6141.
[50] R. Sekirnik, N.R. Rose, A. Thalhammer, P.T. Seden, J. Mecinović, C.J. Schofield, Inhibition of the histone lysine demethylase JMJD2A by ejection of structural Zn(II), Chem. Commun. (2009) 6376–6378.
[51] M. Isaac, J.-M. Latour, O. Sénèque, Nucleophilic reactivity of zinc-bound thiolates: subtle interplay between coordination set and conformational flexibility, Chem. Sci. 3 (2012) 3409–3420.
[52] Z. Chen, J. Zang, J. Kappler, X. Hong, F. Crawford, Q. Wang, et al., Structural basis of the recognition of a methylated histone tail by JMJD2A, Proc. Natl. Acad. Sci. U. S. A. 104 (2007) 10818–10823.
[53] I.L. Alberts, K. Nadassy, S.J. Wodak, Analysis of zinc binding sites in protein crystal structures, Protein Sci. 7 (1998) 1700–1716.
[54] B.L. Vallee, J.E. Coleman, D.S. Auld, Zinc fingers, zinc clusters, and zinc twists in DNA-binding protein domains, Proc. Natl. Acad. Sci. U. S. A. 88 (1991) 999–1003.
[55] L.S. Tsuruda, M.W. Lamé, A.D. Jones, Formation of epoxide and quinone protein adducts in B6C3F1 mice treated with naphthalene, sulfate conjugate of 1,4-dihydroxynaphthalene and 1,4-naphthoquinone, Arch. Toxicol. 69 (1995) 362–367.
[56] D.C. Thompson, K. Perera, R. London, Spontaneous hydrolysis of 4-trifluoromethylphenol to a quinone methide and subsequent protein alkylation, Chem. Biol. Interact. 126 (2000) 1–14.
[57] M. Grugni, M. Cassin, G. Colella, S. De Munari, G. Pardi, P. Pavesi, Indole Derivatives with Antitumor Activity, Eur. Pat. Appl., EP 1835908 A2, (2007).

Please cite this article in press as: M.K.P. Jayatunga, et al., Inhibition of the HIF1α-p300 interaction by quinone- and indandione-mediated ejection of structural Zn(II), European Journal of Medicinal Chemistry (2014), http://dx.doi.org/10.1016/j.ejmech.2014.06.006

[58] N.J. Mabjeesh, D.E. Post, M.T. Willard, B. Kaur, E.G. Van Meir, J.W. Simons, et al., Geldanamycin induces degradation of hypoxia-inducible factor 1alpha protein via the proteosome pathway in prostate cancer cells, Cancer Res. 62 (2002) 2478–2482.
[59] C.E. Stebbins, A.A. Russo, C. Schneider, N. Rosen, F.U. Hartl, N.P. Pavletich, Crystal structure of an Hsp90–geldanamycin complex: targeting of a protein chaperone by an antitumor agent, Cell 89 (1997) 239–250.
[60] S.R. Mooring, B. Wang, HIF-1 inhibitors as anti-cancer therapy, Sci. China Chem. 54 (2011) 24–30.
[61] A.F. Stepan, D.P. Walker, J. Bauman, D.A. Price, T.A. Baillie, A.S. Kalgutkar, et al., Structural alert/reactive metabolite concept as applied in medicinal chemistry to mitigate the risk of idiosyncratic drug toxicity: a perspective based on the critical examination of trends in the top 200 drugs marketed in the United States, Chem. Res. Toxicol. 24 (2011) 1345–1410.
[62] J.B. Baell, G.A. Holloway, New substructure filters for removal of pan assay interference compounds (PAINS) from screening libraries and for their exclusion in bioassays, J. Med. Chem. 53 (2010) 2719–2740.
[63] M. Friedman, Mechanism of the ninhydrin reaction. II. Preparation and spectral properties of reaction products from primary aromatic amines and ninhydrin hydrate, Can. J. Chem. 45 (2011) 2271–2275.
[64] J.L. Santos, P.R. Yamasaki, C.M. Chin, C.H. Takashi, F.R. Pavan, C.Q.F. Leite, Synthesis and in vitro anti *Mycobacterium tuberculosis* activity of a series of phthalimide derivatives, Bioorg. Med. Chem. 17 (2009) 3795–3799.

Please cite this article in press as: M.K.P. Jayatunga, et al., Inhibition of the HIF1α-p300 interaction by quinone- and indandione-mediated ejection of structural Zn(II), European Journal of Medicinal Chemistry (2014), http://dx.doi.org/10.1016/j.ejmech.2014.06.006